Materials Letters 379 (2025) 137710

Contents lists available at ScienceDirect

Materials Letters

journal homepage: www.elsevier.com/locate/matlet

Effect of Sn content on the performance of Nb_3Sn superconducting radio-frequency cavities

Weimin Pan [a,b,*], Peng Sha [a,b,*], Feisi He [a,b], Zhenghui Mi [a,b], Baiqi Liu [a,b], Song Jin [a], Chao Dong [a], Jiyuan Zhai [a,b], Lingxi Ye [a,b], Jinxin Yu [a,b]

[a] Institute of High Energy Physics, Chinese Academy of Sciences, Beijing 100049, China
[b] University of Chinese Academy of Sciences, Beijing 100049, China

ARTICLE INFO

Keywords:
Superconducting radio-frequency
Quality factor
Vapor diffusion
Nb_3Sn
Coating

ABSTRACT

Research of Nb_3Sn superconducting radio-frequency (SRF) cavities was carried out at the Institute of High Energy Physics Chinese Academy of Sciences (IHEP), in order to improve the intrinsic quality factor (Q_0) and accelerating gradient (E_{acc}). Various recipes of coating were attempted at SRF cavities and samples made of Nb, which resulted in different Sn content. It was found that the Sn content, namely the ratio of Nb/Sn, had great influences on the performance of Nb_3Sn SRF cavities. When the ratio of Nb/Sn was slightly higher than 3, the Nb_3Sn SRF cavities showed the best performance during the vertical test. Q_0 of 1.3 GHz 1-cell Nb_3Sn SRF cavity (the ratio of Nb/Sn ≈ 3.16) reached 3.0×10^{10} (@ 4.2 K) and 1.0×10^{11} (@ 2.0 K) at low RF field. This study could provide insights on the effects of Sn content on the performance of Nb_3Sn SRF cavities, which be referenced by the SRF community.

1. Introduction

SRF cavities made of Nb have been widely adopted by large accelerators, such as free electron lasers, synchrotron photon sources, high-energy colliders and proton/neutron sources. However, the Nb SRF cavity has nearly reached its theoretical performance limits at present. Hence, new superconductors beyond Nb are advocated for SRF applications, among which Nb_3Sn is the most promising candidate. During the last decade, SRF cavity made of Nb_3Sn has progressed quickly, which demonstrated much higher Q_0 than Nb [1 –6]. Besides, the superheating field of Nb_3Sn ($B_{sh} \approx 425$ mT) and critical temperature ($T_c \approx 18.3$ K) of Nb_3Sn are much higher than Nb. Hence, Nb_3Sn is the most promising material for SRF application beyond Nb. Many techniques have been attempted to fabricate Nb_3Sn film, e.g., bronze process, chemical vapor deposition (CVD), vapor diffusion and magnetron sputtering. To date, vapor diffusion has been regarded as the most efficient method to synthesize Nb_3Sn, which demonstrates the best performance of Nb_3Sn SRF cavity. Techniques other than vapor diffusion are still in the initial stage, which show much poorer performance. Besides, vapor diffusion is also feasible, through which Nb_3Sn is coated on the Nb substrate. Therefore, it is adopted for the research of Nb_3Sn SRF cavity at IHEP. For the technique of vapor diffusion, the Sn content is critical to the performance of Nb_3Sn SRF cavity. Hence, the optimum ratio of Nb/Sn has been studied by other SRF laboratories, which should be ~ 3 [7,8]. In this paper, the Sn content and performance of Nb_3Sn SRF cavities were investigated. The study indicated that when the ratio of Nb/Sn was slightly higher than 3, the best performance of Nb_3Sn SRF cavities was achieved.

2. The process of vapor diffusion

The process of vapor diffusion was conducted at a dual-vacuum furnace, which was dedicated for coating of Nb_3Sn and introduced in detail [9]. In our study, 1.3 GHz 1-cell SRF cavities made of Nb were adopted as substrate of Nb_3Sn film. The procedure of Nb_3Sn coating is shown as Fig. 1. Sn content was adjusted through the time duration of coating at the highest temperature, which was 1290 °C for crucible and 1130 °C for vacuum chamber. There were six cavities coated in total, as shown in Table 1. The amounts of Sn used were ~ 1 g, which 0.4 ~ 0.5 g for $SnCl_2$. The gate valve of the furnace was always open during the coating process of the three cavities (O1, O2 and O3). For comparison, it was closed during the coating of the other three cavities (C1, C2 and C3), in order to increase the vapor pressure of Sn and $SnCl_2$. Hence, the Sn content should increase.

* Corresponding authors at: Institute of High Energy Physics, Chinese Academy of Sciences, Beijing 100049, China.
E-mail addresses: panwm@ihep.ac.cn (W. Pan), shapeng@ihep.ac.cn (P. Sha).

https://doi.org/10.1016/j.matlet.2024.137710
Received 17 September 2024; Received in revised form 5 November 2024; Accepted 9 November 2024
Available online 12 November 2024
0167-577X/

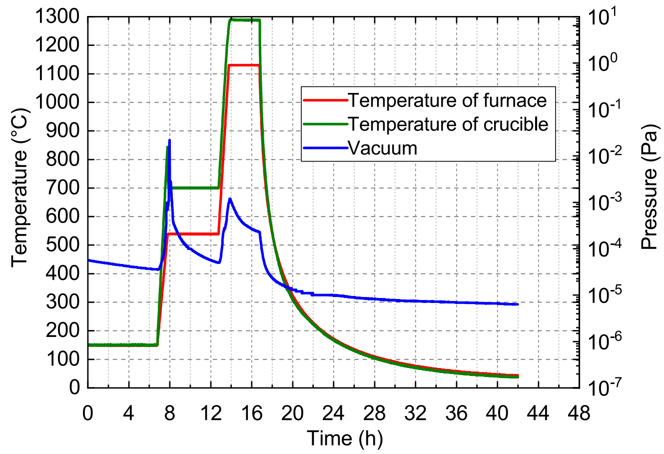

Fig. 1. Temperature and vacuum during the coating process.

Table 1
The recipes of coating process.

Cavity No.	Time duration of coating	Gate valve during coating	Amount of Sn (g)	Amount of $SnCl_2$ (g)	Nb/Sn (Atomic)
O1	1 h	Open	1.0	0.4	3.82
O2	2 h	Open	1.1	0.4	3.48
O3	3 h	Open	1.1	0.4	3.16
C1	1 h	Closed	1.1	0.4	3.19
C2	2 h	Closed	1.1	0.5	2.91
C3	3 h	Closed	1.0	0.5	2.87

3. Results and discussion

The different recipes of coating process in Table 1 were conducted at the samples made of bulk Nb (~ 80 mm × Φ 45 mm), prior to the real cavities. The scanning electron microscopy (SEM) of samples was conducted at Hitachi SU5000/8000, as illustrated in Fig. 2 [10–12]. The Sn content of samples was measured with wavelength dispersive spectrometer (WDS) on EPMA-1720, and the results are shown in Table 1 [13]. For O3 and C1, the ratios of Nb/Sn were close to three. For O2, the ratio was 3.48, which meaned that Sn was not enough. It indicated that the 2-hour coating of O2 might be too short. For C2 and C3, the ratios of Nb/Sn were less than three. Thus, Sn was excessive, which should resulted from closing the gate valve during coating. For O1, the ratio of Nb/Sn was as high as 3.82, which indicated lack of Sn. Besides, the size of Nb_3Sn grain was small (< 1 μm). This was very different from the other recipes, which yielded bigger size (> 1 μm). The grain size was no uniform and there were patchy areas in Fig. 2, which maybe had a bad impact on the RF performance of Nb_3Sn SRF cavity [14,15].

Following coating, the Nb_3Sn cavities were subjected to high-pressure rinsing (HPR), assembly with flanges and leak check in the cleanroom. Afterwards, the Nb_3Sn cavities received vertical RF test [16,17]. The vertical test dewar was well magnetic shielded, so the residual magnetic field was less than 8 mGs. The cool-down rate was > 10 min/K between 22 K and 16 K, and the temperature gap between the top and bottom of the Nb_3Sn SRF cavity was < 0.1 K. Hence, uniform cooling and little thermal gradient were achieved successfully, which were favored for Nb_3Sn SRF cavity.

The vertical test results of Nb_3Sn SRF cavities are shown as Fig. 3. The five cavities (O2, O3, C1, C2 and C3) indicated Q_0 of $\sim 1 \times 10^{10}$ at 4.2 K, which was typical for Nb_3Sn and remarkably higher than Nb ($\sim 6 \times 10^8$). In General, the performance of O2 and O3 was better than C1, C2 and C3. The highest Q_0 at 4.2 K was 3.0×10^{10} at 2.0 MV/m and 1.1×10^{10} at 10.5 MV/m, which were achieved by O3 and O2 respectively. At 2.0 K, O3 exhibited Q_0 of $\sim 1 \times 10^{11}$ at low RF field, which is much higher than O2. It is well known that the surface resistance (R_s) of SRF cavity, which is inversely proportional to Q_0, consists of two components: temperature-dependent BCS resistance (R_{BCS}) and temperature-independent residual resistance (R_{res}). At 2.0 K, R_{BCS} is usually very low and R_{res} dominates for Nb_3Sn. Therefore, it maybe indicated that R_{res} of O3 was low, which had a lower ratio of Nb/Sn than O2. Besides, C2 and C3 demonstrated worse RF performance than C1 at both 4.2 K and 2.0 K, which might result from the excess Sn. In short, it could be preliminary concluded that the ratio of Nb/Sn should be slightly higher than 3 in our coating process, which resulted in better RF performance during the vertical tests.

In addition, the other cavity (O1) only reached the relatively low Q_0 ($< 4 \times 10^9$) at 4.2 K, which was between Nb_3Sn and Nb. In addition, the Q_0 value of O1 at 2.0 K was nearly the same as 4.2 K, which was even lower than the typical Q_0 of Nb ($\sim 1 \times 10^{10}$) at 2.0 K. Considering that

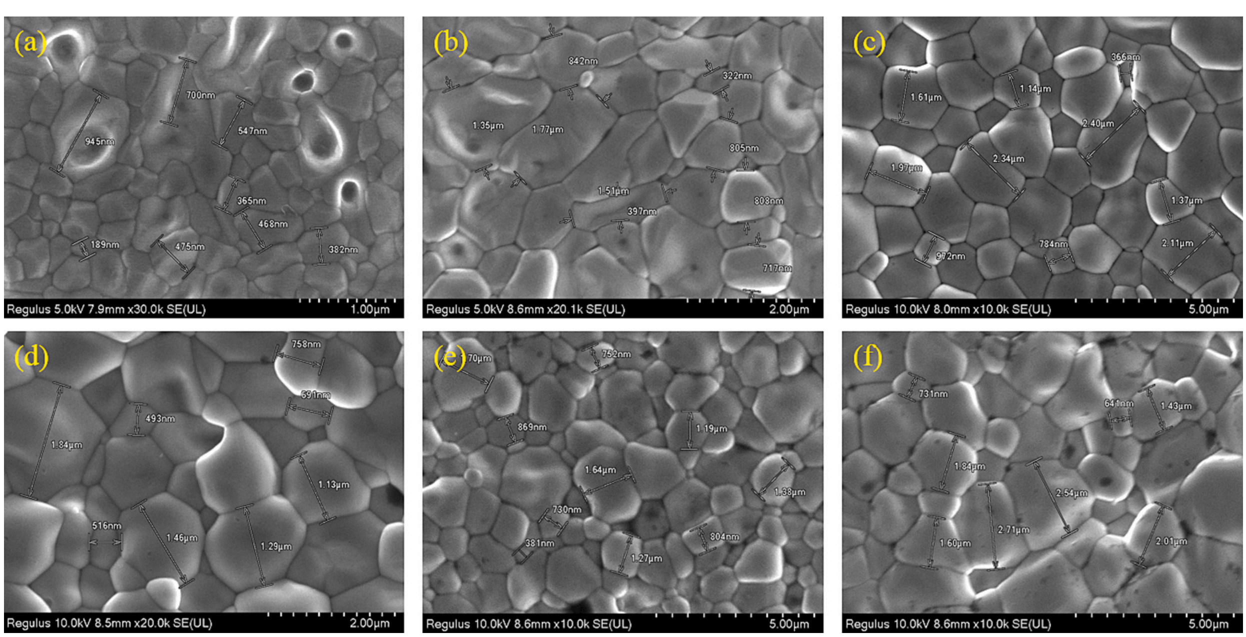

Fig. 2. SEM images of Nb_3Sn samples with different recipes: (a)-O1; (b)–O2; (c)–O3; (d)-C1; (e)–C2; (f)–C3.

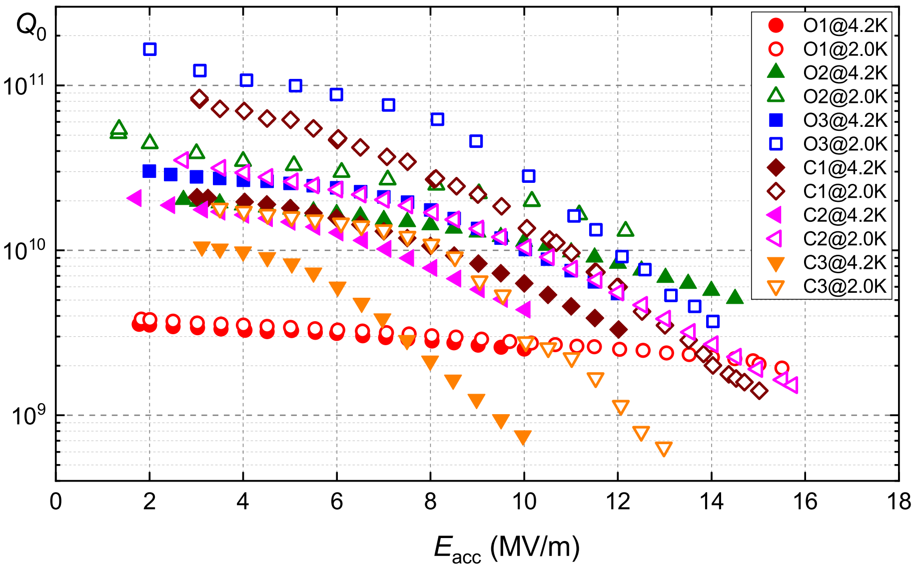

Fig. 3. Vertical test results of 1.3 GHz 1-cell Nb_3Sn SRF cavities (at 4.2 K and 2.0 K).

the ratio of Nb/Sn was 3.82 in Table 1, it was regarded that O1 indicated poor phase of Nb_3Sn because of Sn defficiency.

4. Conclusion

The effect of Sn content on the performance of Nb_3Sn SRF cavities was investigated in this article, which obtained the preliminary results. At 4.2 K, Q_0 of 1.3 GHz 1-cell Nb_3Sn SRF cavity reached 3.0×10^{10} at 2.0 MV/m, which could be further improved. This study could be referenced by the SRF community. In future, the coating process will be further optimized, in order to enhance Q_0 and E_{acc} of Nb_3Sn SRF cavities. Besides, the conduction cooling of Nb_3Sn SRF cavities will be studied, too.

CRediT authorship contribution statement

Weimin Pan: Writing – review & editing, Writing – original draft, Supervision, Project administration, Investigation, Funding acquisition, Conceptualization. **Peng Sha:** Writing – review & editing, Writing – original draft, Visualization, Validation, Software, Funding acquisition, Data curation, Conceptualization. **Feisi He:** Resources, Formal analysis. **Zhenghui Mi:** Methodology, Data curation. **Baiqi Liu:** Software, Methodology. **Song Jin:** Investigation, Formal analysis. **Chao Dong:** Software, Data curation. **Jiyuan Zhai:** Resources, Investigation. **Lingxi Ye:** Software, Data curation. **Jinxin Yu:** Software, Data curation.

Declaration of competing interest

The authors declare that they have no known competing financial interests or personal relationships that could have appeared to influence the work reported in this paper.

Acknowledgements

This research was funded by the National Natural Science Foundation of China (Grant No. 12075270), National Key Programme for S&T Research and Development (Grant No. 2023YFA1606300), the Platform of Advanced Photon Source Technology R&D.

Appendix A. Supplementary data

Supplementary data to this article can be found online at https://doi.org/10.1016/j.matlet.2024.137710.

Data availability

Data will be made available on request.

References

[1] S. Posen, D. Hall, Nb_3Sn Superconducting Radiofrequency Cavities: Fabrication, Results, Properties, and Prospects, Supercond. Sci. Technol. 30 (2017) 033004.
[2] Z. Yang, et al., Low-temperature baking effect of the radio-frequency Nb_3Sn thin film superconducting cavity, Chin. Phys. Lett. 38 (2021) 092901.
[3] K. Takahashi et al., First Nb_3Sn Coating and Cavity Performance Result at KEK. In Proceedings of the 20th International Conference on RF Superconductivity, East Lansing, MI, USA, 28 June–2 July 2021; pp. 27–31, SRF2021.
[4] G. Eremeev, et al., Nb_3Sn multicell cavity coating system at Jefferson Lab, Rev. Sci. Instrum. 91 (2020) 073911.
[5] G. Wang, et al., Nb_3Sn Cavities Coated by Tin Vapor Diffusion Method at Peking University, Applied Sciences. 13 (15) (2023) 8618.
[6] Q. Chen, et al., First Results of Nb_3Sn Coated Cavity by Vapor Diffusion Method at SARI, Coatings 14 (2024) 581.
[7] G. Jiang, et al., Understanding and optimization of the coating process of the radio-frequency Nb_3Sn thin film superconducting cavities using tin vapor diffusion method, Applied Surface Science 643 (2024) 158708.
[8] S. Posen, Understanding and overcoming limitation mechanisms in Nb3Sn superconducting RF cavities, Cornell University, 2015. PhD thesis.
[9] C. Dong, et al., Preliminary Research of Niobium Cavity Coating with Nb_3Sn Film at IHEP, Physica c: Superconductivity and Its Applications 600 (2022) 1354107.
[10] L. Shao, et al., Effect of Cold-Spray Parameters on Surface Roughness, Thickness and Adhesion of Copper-Based Composite Coating on Aluminum Alloy 6061 T6 Substrate, Processes 11 (2023) 959.
[11] W. Li, et al., Effects of spraying parameters and heat treatment temperature on microstructure and properties of single-pass and single-layer cold-sprayed Cu coatings on Al alloy substrate, Surf. Coat. Technol. 131184 (2024).
[12] L. Guo, et al., Theoretical design and experimental verification of high-entropy carbideablative resistant coating, Advanced Powder Materials 3 (2024) 100213.
[13] M. Cui et al., Applications of laser-induced breakdown spectroscopy in industrial measurement and monitoring: Multi-technology combination. Applied Spectroscopy Reviews, September, 1–49, 2024.
[14] G. Zhou et al., "An RF Amplifier Circuit for Enhancement of Echo Signal Detection in Bathymetric LiDAR," in IEEE Sensors Journal, vol. 22, no. 21, pp. 20612-20625, 1 Nov.1, 2022.
[15] P. Wen, et al., Synthesis design of high-selectivity wideband balanced bandpass filterbased on parallel coupled lines, AEU - International Journal of Electronics and Communications 176 (2024) 155159.
[16] C. Wang, et al., Terahertz dual-band bandpass filter based on spoof surface plasmon polaritons with wide upper stopband suppression, Opt. Express 32 (2024) 22748–22758.
[17] P. Wen, et al., Direct Synthesis of Continuously Tunable Wideband Bandpass Filtering Attenuator With Multiple Transmission Zeros, IEEE Transactions on Circuits and Systems II: Express Briefs 71 (9) (Sept. 2024) 4346–4350.